Front. Chem. China 2009, 4(2): 149–153
DOI 10.1007/s11458-009-0035-6

RESEARCH ARTICLE

Liangzhun YANG, Lanfen ZHANG, Jun CHEN, Liwen REN
Yanting ZHU, Xiuying WANG, Xibin YU

Study on the fluorescence and thermal stability of hybrid materials $Eu(Phen)_2Cl_3$/MCM-41

Abstract A series of luminescent hybrid materials $Eu(Phen)_2Cl_3$/MCM-41 that the different assembled mass of $Eu(Phen)_2Cl_3$ included into the channels of MCM , have been synthesized by combining ultrasound technology. The properties of the hybrid materials were characterized by XRD(X-ray Diffraction), N_2-adsorption-desorption, FT-IR and luminescence spectrum. The results show that the rare-earth compounds had been loaded into the holes of mesoporous material MCM-41. The luminescence intensities of the hybrid materials were improved as the increase of the loading concentration of the rare-earth complexes. The hybrid material has the maximal luminescence intensity when it reached the saturated loading concentration (7.17%). To compare with the pure rare-earth complex, the thermal stability of the hybrid materials were enhanced by about 100°C.

Keywords Eu(III) complexes, MCM-41, hybrid materials, fluorescence, thermal stability

1 Introduction

As a kind of high-performance light-emitting materials, rare-earth organic complexes are one of significant photoactive materials [1–3]. However, the advantages cannot be adequately employed because of the instability of these organic complexes that decomposed in the light and heat conditions. It is supposed that combining the rare-earth organic complexes and the inorganic materials that have high optical, thermal and chemical stabilities may resolve this problem. The mesoporous material MCM-41 can be a candidate with orderly honeycomb-like porous structure and has been used to improve properties of rare-earth organic complexes. The structural array of MCM-41 is composed of one-dimensional linear holes and heaped as the hexagonal close packed structure. The typical hole diameter is about 4 nm, and can be modulated between 1.5–10 nm. Furthermore, with its high specific surface area (1000 m/g or so) as well as the absorption capacity (> 0.7 mL/g), MCM-41 performs a valuable role in catalysis, absorption or separation, the fixing of enzymes and the fabrication of nano-optoelectronic devices [4].

It has been reported that the rare-earth complexes are assembled into the molecular sieve MCM-41 to form light-emitting composite materials. However, the problems such as the low loading concentration of rare-earth complexes in the pores of MCM-41 and the low emission intensity of the composite materials still exist [5–7].

Ultrasound technology as an assistant method for material preparation has been gradually noticed. Using the ultrasonic cavitation role, i.e. the physical and chemical effect produced from the vibration, growth, shrinkage and breakdown of the micro air bubble in the solution under the acoustic field, which can accelerate the material transfer and dispersal, the capability of material can be improved [8].

In this paper, methanol was used as solvent, assistant by ultrasound technology, to assemble the high performance of light-emitting rare-earth complexes Eu $(Phen)_2$ Cl_3 into the pore structures of MCM-41. As a result, high fluorescence performance and thermal stability hybrid material was obtained, in which loaded concentration was as high as 7.17%.

2 Experimental

2.1 Reagents and Equipments

Eu_2O_3 (99.99%, Res Group of Chemical Reagents Ltd.), 1,10-Phenanthroline monohydrate ($Phen \cdot H_2O$, AR, Shanghai Third Chemical Reagent Factory), Hexadecyltrimethyl ammonium bromide (CTAB, AR, China Medicine Shanghai Chemical Reagent Co.), tetraethyl

Translated from *Chemical Research and Application*, 2008, 20(1) (in Chinese)

Liangzhun YANG (✉), Lanfen ZHANG, Jun CHEN, Liwen REN, Yanting ZHU, Xiuying WANG, Xibin YU
Department of Chemistry, Shanghai Normal University, Shanghai 200234, China
E-mail: ssdylz@shnu.edu.cn

orthosilicate (TEOS, AR, Shanghai First Chemical Reagent Factory), concentrated ammonia (CP, Shanghai Zhenxin Second Factory), absolute ethanol (AR, Shanghai First Chemical Reagent Factory).

The content of C, H and N was measured by the 2400 Perkin Elmer elemental analyzer. The content of Eu(III) in the hybrid material was characterized by the Inductively Coupled plasma (ICP) Atomic Emission Spectrometer (ICP-OES VISTA-MPX, Varian). The XRD pattern was tested by the Rigaku D/MaxIIIB diffractometer. The N_2-adsorption-desorption isotherms and the distribution of the pore size of the hybrid material were measured by a high-speed automated specific surface area and pore size analyzer (NOVA 4000e). The FT-IR spectra and PL spectra were measured by the Nicolet Avatar 370 DTGS and Varian Cary-Eclipse 500, respectively.

2.2 Synthesis of MCM-41

A given amount of CTAB was first mixed with ammonia solution in a flask with a magnetic stirrer. A certain amount of TEOS was then added into the mixed solution slowly. The molar ratio of CTAB:TEOS:NH_3 was in 1:2:52 (in Molar). This flask was put in a water bath at 50°C and stirred for 4 h, and then MCM-41 precursors were collected by centrifugation, washed, and dried at 60°C in a vacuum oven for 4 h. The precursor was calcined at 550°C for another 5 h, and the product, MCM-41, was obtained.

2.3 Synthesis of complex $Eu(Phen)_2Cl_3$

Eu_2O_3 was dissolved in hydrochloric acid to form the europium chloride solution and then this solution was vaporized to get crystal europium chloride. Later, when $EuCl_3$ was dissolved completely in a little distilled water, absolute alcohol was added to form 0.1 mol·dm^{-3} Eu^{3+} (solution I). Additional, Phen·H_2O was dissolved in absolute alcohol to form 0.1 mol·dm^{-3} Phen (Solution II). The two of above solutions (I and II) were mixed according to a volume ratio in 1:2, and then the mixed solution were kept in a 50°C water bath and reacted for 2 h. After the precipitates were collected by centrifugation, they were washed with ethanol and dried at 120°C under vacuum. White powdery products were obtained. Elemental analysis: found 44.15(C), 3.25(H), 8.62(N), 23.43(Eu); calculated for $Eu(Phen)_2Cl_3 \cdot 2H_2O$ 44.03(C), 3.08(H), 8.46(N), 23.21(Eu).

2.4 Assembling the hybrid material $Eu(Phen)_2Cl_3$/MCM-41

A flask with 0.05 g $Eu(Phen)_2Cl_3$ added into 25 mL absolute methanol and ultrasonic reaction for 15 minutes until the complexes were totally dissolved. Then, 0.5 g MCM-41 was added and the mixtures were placed in an ultrasonic instrument to react for 2 h and then stirred at room temperature for 10 h. The resulting precipitates were washed repeatedly by using absolute methanol until the filter liquor irradiated by UV lamp peaked at 254 nm shows no red-emitting signs. The precipitates was followed by drying at 100°C in a vacuum drying oven until the weight of the products were kept constant. The mass percent of the rare-earth complex $Eu(Phen)_2Cl_3$ assembled into the molecular sieve MCM-41 was calculated according to the content of Eu(III) in the hybrid material (measured by the ICP). At the same time, a series of methanol solution of complex in different concentrations and same volumes were prepared for synthesizing the hybrid materials with the different assembled amounts.

Since the hybrid materials with the different assembled amount had the similar XRD pattern, PL spectrum, FT-IR spectrum and UV-Vis spectrum, just the peak intensities were different, so that, the figures of $Eu(Phen)_2Cl_3$/MCM-41(7.17%) are only shown in this article.

3 Results and discussion

3.1 XRD analysis

Figure 1 presents the XRD patterns of MCM-41 and $Eu(Phen)_2Cl_3$/MCM-41. It was clearly shown that Fig. 1a represented the three distinct diffraction peaks indexed as (100), (110) and (200) in the low 2θ region of 1°–5°, which were the characteristic peaks of MCM-41 mesoporous phase [9]. The MCM-41 not only has the much stronger (100) peak than that of the $Eu(Phen)_2Cl_3$/MCM-41, but also both (110) and (200) diffraction peaks were distinct. It indicated that the arrangement of the channels in structure of MCM-41 was in highly ordered [5]. After the $Eu(Phen)_2Cl_3$ was assembled into the sieve MCM-41, the position of (100) peak remained unchanged, but its intensity decreased apparently and the peak became broad. In addition, the (110) and (200) reflection peaks disappeared. We could conclude that the assembling process had no effect on the crystal form of MCM-41.

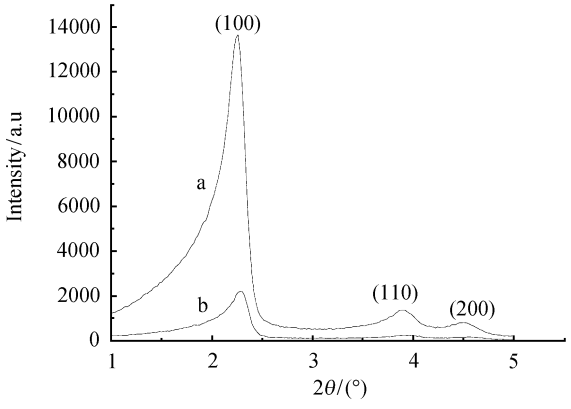

Fig. 1 XRD patterns of MCM-41 (a) and $Eu(Phen)_2Cl_3$/MCM-41 (b)

The presence of $Eu(Phen)_2Cl_3$ inside the pores of $Eu(Phen)_2Cl_3$/MCM-41 made the order of the channels in structure of MCM-41 decrease remarkably.

3.2 N_2-adsorption-desorption analysis

The textural properties derived from nitrogen adsorption–desorption measurements are summarized in Table 1. It can be seen from Table 1 that the specific surface area, pore volume and average pore diameter of $Eu(Phen)_2Cl_3$/MCM-41(7.17%) were sharply reduced compare with that of MCM-41. It indicated that the complexes have been embedded into the channels of the MCM-41.

Table 1 Parameters of MCM-41and $Eu(Phen)_2Cl_3$/MCM-41 measured by N_2 adsorption–desorption isotherms

Samples	BET specific surface area /($m^2 \cdot g^{-1}$)	Average pore diameter /nm	Pore volume/($mL \cdot g^{-1}$)
MCM-41	1040	3.42	0.89
$Eu(Phen)_2Cl_3$/MCM-41	874.3	3.21	0.70

Figure 2 shows the N_2 adsorption-desorption isotherms of MCM-41 and $Eu(Phen)_2Cl_3$/MCM-41. From the two branches of adsorption-desorption isotherms, the presence of a sharp adsorption jump/desorption drop with hysteresis in the P/P_0 region from 0.25 to 0.4 shows that the both of molecular sieve and hybrid material possessed the characteristic mesoporous structure. The steep rise was related to the pore-size of the sample [10]. The higher the numerical value of jump point (P/P_0) is, the bigger pore size of the sample will be. Moreover, the slope of jump was associated with the uniformity of pore size of the sample. With the increase of the degree of abrupt change, the sample will show a very narrow pore-size distribution and a greater increase of the pore volume. The results demonstrated that as the complexes have been embedded into the channels of MCM-41, the pore volume and the uniformity of pore channels of MCM-41 were decreased. This was consistent with XRD analysis.

3.3 The analysis of the percent mass of $Eu(Phen)_2Cl_3$ in the hybrid materials

To study the maximum content of the complexes that could be assembled into the molecular sieve, we changed the concentration of the complex in the methanol solution and prepared a series of the hybrid materials by the same synthesis method (see Section 2.4). The results are presented in Table 2. It can be seen from Table 2 that the content of the complexes assembled into the channels of MCM-41 was increased with the increase of the concentration of the complexes in methanol solution when the concentration was less than 0.008 g/mL. When the concentration of $Eu(Phen)_2Cl_3$ was 0.008 g/mL, the content of the assembled complexes was 7.17%. To further increase in concentration of $Eu(Phen)_2Cl_3$, the content of the assembled complexes remained basically unchanged. This was clearly shown that the maximum assembled content was about 7.17%.

Table 2 The percent mass of $Eu(Phen)_2Cl_3$ in the hybrid materials

The concentration of $Eu(Phen)_2Cl_3$ in methanol /(g/mL)	0.002	0.004	0.006	0.008	0.010
Measured *m*/%	4.52	5.12	6.11	7.17	7.19

3.4 The spectrum of FT-IR

Figure 3 showed the FT-IR spectra of Phen, $Eu(Phen)_2Cl_3$, MCM-41 and $Eu(Phen)_2Cl_3$/MCM-41. It can be observed from Fig. 3 that the FT-IR spectrum of the free Ligand Phen shows the characteristic absorption bands at 1622 cm^{-1} ($\delta_{C=N}$), 850 cm^{-1} ($\delta_{C\text{-}H}$) and 743 cm^{-1} ($\delta_{C\text{-}H}$). The

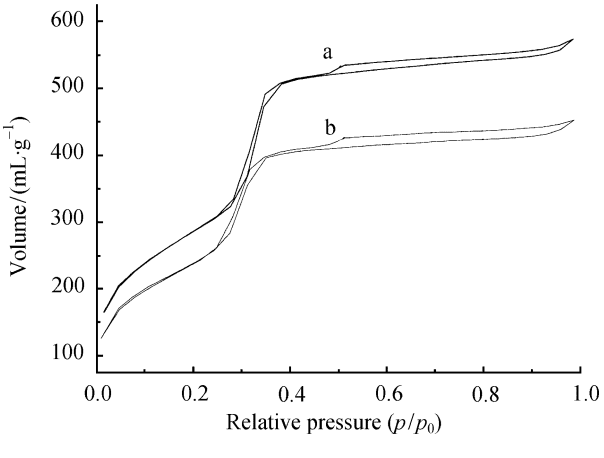

Fig. 2 N_2 adsorption-desorption isotherms of MCM-41 (a) and $Eu(Phen)_2Cl_3$/MCM-41 (b)

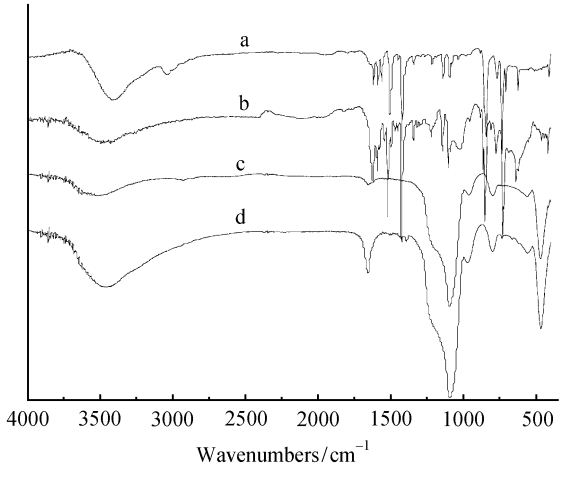

Fig. 3 FT-IR spectra of Phen (a), $Eu(Phen)_2Cl_3$ (b), MCM-41 (c) and $Eu(Phen)_2Cl_3$/MCM-41 (d)

characteristic peaks of pure Phen red-shift to 1591 cm^{-1}, 840 cm^{-1} and 722 cm^{-1}, respectively, because of the complex formation. It showed that the coordinate bonds have formed between the Eu^{3+} ions and nitrogen atom in Phen [11]. The FTIR spectrum [Fig. 3(c)] of MCM-41 showed a broad and strong absorption peak, assigned to the symmetric stretching vibration modes of the mesoporous framework (Si–O–Si) at around 1095 cm^{-1}, bands at 798 and 465 cm^{-1}, assigned to the Si–O–Si bending vibrations [12]. As can be seen from Fig. 3(d), assembled complexes, there also present the Si–O–Si stretching vibrations and bending vibrations in the FTIR spectrum of the hybrid material $Eu(Phen)_2Cl_3$/MCM-41(7.17 %). The results indicated that the mesoporous structure still existed in the samples. Moreover, the polarity of the hybrid material increased as $Eu(Phen)_2Cl_3$ embedded into the channels of MCM-41, which can significantly increase the peak intensity [13].

3.5 PL Spectrum

Figure 4 shows the excitation and emission spectra of the samples. In general, the emission bands of Eu^{3+} were due to the transitions of $^5D_0 \rightarrow {}^7F_1$ and $^5D_0 \rightarrow {}^7F_2$. It can be clearly observed that the magnetic dipole transition located at about 590 nm corresponds to $^5D_0 \rightarrow {}^7F_1$ of Eu^{3+} ions and the ambience of Eu^{3+} is little impact to the magnetic dipole transition. The electronic dipole transition, located at about 613 nm, corresponds to $^5D_0 \rightarrow {}^7F_2$ of Eu^{3+} ions and the electric dipolar $^5D_0 \rightarrow {}^7F_2$ transition is very sensitive to the ambience of Eu^{3+}. If Eu^{3+} ions were located in the inversion center lattices, it mainly could show magnetic dipole $^5D_0 \rightarrow {}^7F_1$ transition, which had the same rule as the free ions. If Eu^{3+} ions were located in the non-inversion center lattices, the forbidden transition was unchained, it mainly shows the electronic dipole $^5D_0 \rightarrow {}^7F_2$ transition [14].

As shown in Fig. 4, since the $Eu(Phen)_2Cl_3$ has been embedded into the channels of MCM-41, Eu^{3+} ions deviate from the central symmetry and the symmetry of lattices decreased, the forbidden transition was unchained, so the emission intensity from electronic dipole $^5D_0 \rightarrow {}^7F_2$ transition was increased in the hybrid material $Eu(Phen)_2Cl_3$/MCM-41. The inset in Fig.4 showed that the intensity of emission spectra was increased with the increase of the assembled content of the complexes. When the content of the complexes assembled into the channels of MCM-41 increased to saturation (7.17%), the fluorescence intensity of $Eu(Phen)_2Cl_3$/MCM-41 reached the maximum.

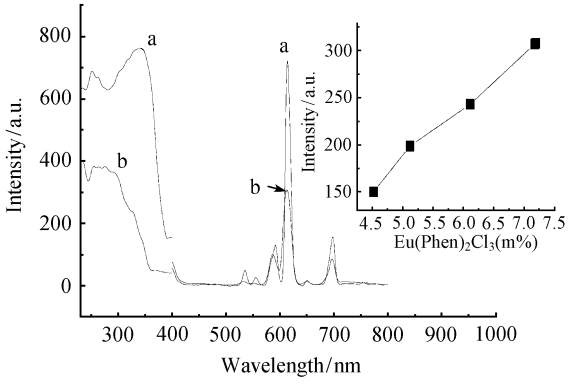

Fig. 4 The excitation and emission spectra of $Eu(Phen)_2Cl_3$ (a) and $Eu(Phen)_2Cl_3$/MCM-41 (b)
(The inset is the emission spectra of hybrid materials in 613 nm with different content rare-earth complex)

3.6 The thermal stability

The relationships between relative emission intensity at 613 nm and the heat treatment temperatures of the samples, after $Eu(Phen)_2Cl_3$ and $Eu(Phen)_2Cl_3$/MCM-41 heated treatment for 2 h at different temperatures, were investigated and the results as shown in Fig. 5. It was shown that the residual water in samples being gradually evaporated and a steady increased in emission intensity with increasing heat treatment temperature, because water has a part of the fluorescence quenching effects on the rare-earth ions. When the heat treatment was over 300°C, a sharp decline of the fluorescence of $Eu(Phen)_2Cl_3$ was observed. This can be ascribed to decomposition of the rare earth complexes. However, the fluorescence intensity of $Eu(Phen)_2Cl_3$ assembled into the molecular sieve MCM-41 began to decrease until the temperature was as high as 400°C. It shows that the thermal stability of $Eu(Phen)_2Cl_3$/MCM-41 increased by about 100°C to compare with the pure $Eu(Phen)_2Cl_3$.

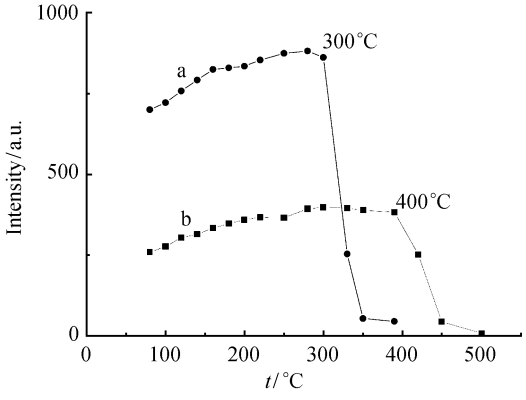

Fig. 5 The influence of heat treatment temperature on the relative emission intensity in 613 nm of $Eu(Phen)_2Cl_3$ (a) and Eu $(Phen)_2Cl_3$/MCM-41 (b)

4 Conclusion

A series of luminescent hybrid materials $Eu(Phen)_2Cl_3$/MCM-41, with different assembled mass of $Eu(Phen)_2Cl_3$, have been synthesized by combined with ultrasound technology. The research results show that the fluorescent

intensity of hybrid materials was increased with the increase of the assembled content of $Eu(Phen)_2Cl_3$. When the content of the complexes assembled into the channels of MCM-41 came to saturation (7.17%), the fluorescence intensity of $Eu(Phen)_2Cl_3$/MCM-41 reached the maximum. Compared with the pure $Eu(Phen)_2Cl_3$, the thermal stability of $Eu(Phen)_2Cl_3$/MCM-41 increased by about 100°C.

Acknowledgements This work was supported by Shanghai Normal University Fund (SK200843); the Science and Technology Development Fund, Shanghai, China (Project Nos. 04JC14089 and 05JC14074).

References

1. Yan B, Zhang H J, Wang S B, Ni J Z. The synthesis, characterization and photophysical properties of binary and ternary rare earth complexes with N phenylanthranilic acid and 1,10 phenanthroline. Chemical research in chinese universities, 1998, 19 (5): 671–675
2. Hu M L, Huang Z Y, Cheng Y Q, Wang S, Lin J J, Hu Y, Xu D J, Xu Y Z. Crystal structure and fluorescence spectrum of the complex [Eu (III) (TTA)$_3$(phen)]. Chinese Journal of Chemistry, 1999, 17 (6): 637–643
3. Zhang Y, Jin L P, Lu S Z. Crystal structure and luminescence of Eu $(BA)_3$phen complex. Journal of The Chinese Rare Earth Society, 1998, 16 (1): 5–8
4. Liu F Y, Fu L S, Lin J, Zhang H J, Wang S B, Xu Q H, Ding H, Zou Y C. Synthesis and characterization of a novel hybrid inorganic-Organic mesoporous luminescent material $(phen)_2Eu$/MCM-41. Chinese Journal of Applied Chemistry, 2001, 18(5): 380–383
5. Xu H Y, Guan J Q, Wu S J, Kan Q B. Synthesis of Beta/MCM-41 composite molecular sieve with high hydrothermal stability in static and stirred condition. Journal of Colloid and Interface Science, 2008, 329: 346–350
6. Yin W, Zhang M S, Kang B S. Encapsulation of the functional supramolecular NSM of rare earth and its comparison of fluorescence. Chinese Journal of Inorganic Chemistry, 2001, 17 (1): 60–63
7. Fu L S, Zhang H J. Preparation, characterization and luminescent properties of MCM-41 type materials impregnated with rare earth complex. Mater Sci Technol, 2001, 17(3): 293–298
8. Fang M, Yang L Z, Liu C,, Wang X Y, Yu X B. Preparation and properties of luminous material of $CaSiO_3$:(Pb, Mn) by ultrasonic wave-assisted sol-gel method. Chemical Research and Application, 2007, 19(2): 140–144
9. Park S E, Kim D S, Chang J S, Kim WY. Synthesis of MCM-41 using microwave heating with ethylene glycol. Catalysis Today, 1998, 44: 301–308
10. Yuan C Z, Gao B, Su L H, Zhang X G. Interface synthesis of mesoporous MnO_2 and its electrochemical capacitive behaviors. Journal of Colloid and Interface Science, 2008, 322: 545–550
11. Wang Z X, Chen H, Tan M J, Shu W G. The synthesis and fluorescence properties of Doping Europium-Benzonic Acid-Phenanthroline complexes. Spectroscopy and Spectral Analysis, 2005, 25(7): 1106–1109
12. Wu C, Chen W, Zhou J, Tian G, Zhao C X. Preparation and Characterization of Eu/MCM-41 Mesoporous Composite Material. Journal of The Chinese Rare Earth Society, 2005, 23 (2): 175–178
13. Chen J, Song Q Z. Organic Spectrum Analysis. Beijing: The Publishing House of Beijing Institute of Technology, 1996, 47–48
14. Meng Q G, Lin J, Fu L S, Zhang H J, Wang S B, Zhou Y H. Sol-gel deposition of calcium silicate red-emitting luminescent films doped with Eu^{3+}. Journal of Materials Chemistry, 2001, 11: 3382–3386